Journal of Translational Medicine

RESEARCH

Open Access

FACS-Proteomics strategy toward extracellular vesicles single-phenotype characterization in biological fluids: exploring the role of leukocyte-derived EVs in multiple sclerosis

Maria Concetta Cufaro[1,2], Paola Lanuti[2,3], Domenico De Bellis[2,3], Serena Veschi[4], Anna Piro[4], Antonella Fontana[4], Alice Di Sebastiano[2,5], Davide Brocco[6], Pasquale Simeone[2,3], Serena Pilato[4], Reza M. H. Khorooshi[7], Valentina Tomassini[8], Marianna Gabriella Rispoli[8], Luca Federici[1,2], Ilaria Cicalini[1,2], Damiana Pieragostino[1,2] and Piero Del Boccio[2,5*]

Abstract

Background The isolation and proteomics characterization of extracellular vesicles (EVs) from body fluids is challenging due to their vast heterogeneity. We have recently demonstrated that Fluorescence-activated Cell Sorting (FACS) efficiently isolates the whole EV circulating compartment directly from untouched body fluids enabling a comprehensive EV proteomics analysis.

Results Here, we characterized, for the first time, a single-phenotype EV subset by sorting leukocyte-derived EVs (Leuko EVs) from peripheral blood and tears of healthy volunteers. Using an optimized and patented staining protocol of the whole EV compartment we identified and excluded non-EV particles, debris and damaged EVs. We further isolated, using an anti-CD45 antibody, Leuko EVs (CD45+ EVs), reaching a high level of purity (> 90%). Purified Leuko EVs were characterized using atomic force microscopy, nanoparticle tracking, and shotgun proteomics analysis revealing a similar coded protein cargo in both biological fluids. Subsequently, the same workflow was applied to tears from Relapsing–Remitting Multiple Sclerosis (RRMS) patients, revealing a Leuko EVs protein cargo enrichment that reflects the neuroinflammatory condition characteristics of RRMS. This enrichment was evidenced by the activation of upstream regulators *TGFB1* and *NFE2L2*, which are associated with inflammatory responses. Additionally, the analysis identified markers indicative of endothelial cell proliferation and the development of enhanced vascular networks, with *AGNPT2* and *VEGF* emerging as activated upstream regulators. These findings indicate the complex interplay between inflammation and angiogenesis in RRMS.

Conclusions In conclusion, our combined FACS-Proteomics strategy offers a promising approach for biomarker discovery, analysing cell-specific EV phenotypes directly from untouched body fluids, advancing the clinical value

*Correspondence:
Piero Del Boccio
piero.delboccio@unich.it
Full list of author information is available at the end of the article

of tears EVs and improving the understanding of EV-mediated processes in vivo. Data are available via ProteomeXchange with the identifier PXD049036 and in EV-TRACK knowledgebase with ID: EV240150.

Keywords Leukocyte-derived extracellular vesicles, Multiple sclerosis, Proteomics, Tears, EV fluorescence activated cell sorting isolation

Background

Isolation and characterization of extracellular vesicles (EVs) from biological samples remain a technological challenge even if several improvements have been recently achieved. Circulating EVs in biological fluids are an extremely heterogeneous compartment in terms of sizes and phenotypes since they are released from different cell types and it is well known that cells release EVs with specific molecular cargoes in term of proteins, lipids/metabolites, RNAs and DNA fragments, depending on their role and the individual physio-pathological condition [1, 2]. It is becoming increasingly clear that the intercellular information exchange mediated by EVs displays potent regulatory functions, mediated both by their surface receptors and their content [3]. EVs are emerging as relevant players in the inter-cellular crosstalk and in different pathophysiological conditions [4, 5], given that they convey materials dynamically related to the status of their parental cells. Furthermore, EVs were identified in all body fluids, such as cerebrospinal fluid (CSF), tears, saliva, urine, milk, and peripheral blood (PB) [2, 6–8]. Therefore, isolating EVs from body fluids and analyzing their biological content represents, today, a stimulating challenge to improve our knowledge on EV biology.

Nowadays, the characterization of proteome has been dramatically accelerated thanks to the technological improvements of the liquid chromatography coupled to tandem mass spectrometry (LC–MS/MS) platforms, which are useful to understand the phenotype and the role of EVs even in complex biological matrices unraveling key factors biological pathway modulations [9, 10].

Nevertheless, the EV isolation step, not yet standardized, represents one of the main issues in EV proteomics characterization, particularly affected by biological fluid soluble proteins cross-contaminations. Moreover, isolated EVs could be "coated" with proteins, glycoproteins or glycolipids likely to cause aggregation, fusion and co-sedimentation of similar vesicles, negatively affecting the recovery, purity, and further molecular analyses. Another relevant issue concerns the vast heterogeneity of the circulating EV population in terms of phenotypes since each single cell type releases specific EVs, biologically different from those released by other cell types [11]. Ideally, the best EV isolation method, not only for proteomics characterization, should be able to minimize soluble contaminants and allow to collect separately the different EV phenotypes based on their cell of origin.

Giving a brief overview of principal EV isolation protocols, the most used are based on differential or density gradient centrifugation [11, 12]. Other studies employed the use of chemical precipitation kits [13, 14], or several series of ultrafiltration combined with ultracentrifugation or size-exclusion chromatography (SEC) [15, 16], or immuno-isolation with magnetic beads like ExoChip [17], and microfluidic separations with ciliated micropillars [18]. Moreover, recently, various isolation and detection methods have been combined simultaneously [19, 20] improving final performances.

Despite several attempts, the best strategy for EVs isolation from biological fluids remains an open question for the scientific community, especially looking at their suitability for proteomics application. Isolated EVs may be used as liquid biopsy allowing a huge reduction of the high dynamic range of protein concentration detectable in whole biofluids, making them a promising candidate for biomarker discovery in the so called "dark proteome" [21]. Their circulating proteome may reveal an underappreciated world to investigate, suggesting that their molecular cargo may reflect pathophysiological conditions of the Central Nervous System (CNS) considering that distinct types of brain cells release EVs which function as shuttles to deliver their cargo among different cells [22]. For example, in the context of multiple sclerosis, EVs can drive both inflammatory processes and immune tolerance, which are typical characteristics of such immune-mediated demyelinating disorder [23]. Many studies have been conducted on multiple sclerosis EVs molecular cargo characterization, revealing specific membrane markers for endothelial-derived EVs (i.e., CD31 (PECAM-1), CD51 (integrin), CD54 (ICAM-1), CD62E (ELAM-1 or E-selectin), CD63E, and CD105 (endoglin) that increases the adhesion of inflammatory leukocytes to endothelial cells and promotes their transendothelial migration into the CNS), and leukocyte-derived EVs (C-C chemokine receptor type 3 (CCR3) and type 5 (CCR5), unravelled as specific markers of T cells in CSF) [24]. Moreover, patients have exhibited a strong increase of serum myelin basic protein (MBP) levels compared to healthy people, demonstrating a potential crosstalk between EVs released by oligodendrocytes and

microglia with demyelinating processes [25]. Altogether, EV protein cargo reveals specific molecules involved in neurodegeneration and demyelination, for example acid sphingomyelinase (aSMase) was highly expressed in CSF of relapsing–remitting multiple sclerosis (RRMS) patients, correlating with EVs release [26]. Plasma kallikrein (KLKB1), dickkopf-related protein 3 (DKK3), complement component C6 (C6), and protein S100A9 were identified in EVs CSF of RRMS subjects confirming their role in wound healing, homeostasis, and coagulation, such as fibrinogens which can promote the autoimmunity and inflammatory demyelination disorders [27, 28].

Within such a complex and dynamic scenario, we have recently optimized an innovative protocol for the isolation and proteomics characterization of EVs directly from unprocessed biofluids. The FACS-based purification method takes advantage of the combination of the lipophilic cationic dye (LCD) and phalloidin for the identification of damaged membranes (patent codes: 10,201,800,000,398; EP19164567A·2019-03-22). By applying this protocol, a high level of repeatability in terms of EV counts was achieved. We previously demonstrated that EVs isolated by such a strategy were purified from the most abundant contaminants (i.e., non-EV particles), such as albumin and apolipoprotein when EVs from peripheral blood were purified [29]. As a result, we were able to probe and purify LCD+/Phalloidin- intact EVs suitable for proteomics characterization [29]. The first application of such an innovative "FACS-Proteomics" workflow was the study of total EV pools (label free) from untouched CSF and tears collected from RRMS patients, revealing a proteins cargo involved in inflammation, angiogenesis and immune response signalling in both biofluids [30].

We demonstrated that tear analysis can be extended beyond the ocular disease since they contain enriched biological molecules filtrated from circulatory system, representing a precious source of information in physiological and pathological conditions. This concept was elegantly strengthened by Hu et al. in a recent paper in which they found the genesis of tear EV proteins with 37 tissues and 79 cell types by using universal analysis in combination with the Human Protein Atlas consensus dataset [31].

Here, we reported a first application of the recently optimized FACS-Proteomics workflow in the proteomics characterization of EV single-phenotype (labelled) from untouched body fluids. As a proof of concept, we characterized the protein cargo of leukocyte-derived EVs (Leuko EVs) isolated from blood and tears of healthy subjects. Finally, we carried out a label free proteomics analysis on Leuko EVs purified from tears of RRMS patients, proving that the leukocyte's role in a such autoimmune disease, may be, at least in part, EV-mediated.

Methods

Ethics statement

The study design was made following the protocol approved on 29 December 2020 by the Ethic committee of "G. d'Annunzio" University, in accordance with the Declaration of Helsinki (World Medical Association, 1997). All enrolled people were informed about the procedures and provided written informed consent to participate in the study.

Recruitment and sample collection

Subjects enrolled as Healthy donors (HCs) were selected with no prior history of systemic disease or administration of immunosuppressing or immunomodulating drugs (n = 10). RRMS patients were enrolled at the Multiple Sclerosis Centre of "SS. Annunziata" Hospital, Chieti (Italy) after that their clinical diagnosis was confirmed by magnetic resonance imaging (MRI) studies and by the presence of oligoclonal bands (OCBs) in CSF fulfilling the 2017-revised McDonald diagnostic criteria. 23 RRMS patients with the same characteristics (i.e., diagnosis of RRMS according to the 2017-revised McDonald criteria) were focused on the proteomics characterization of Leuko EVs cargo (Table 1). All RRMS patients were in clinical remission (i.e., they did not experience relapses within the 30 days prior to sample collection nor were

Table 1 Clinic-demographic characteristic of subjects enrolled for sorting Leuko-derived EVs for proteomics assessment

Clinical-demographic characteristics	RRMS (n = 23)	HCs (n = 10)
Age	41.9 ± 11.6	31.4 ± 4.42
Sex (female), %	86.96%	60%
Disease duration, years	12.7 ± 10.3 n.a	n.a
EDSS score, median (range)	3.5 (range: 1–7)	n.a
Patients with ≥ 1 relapse in the previous year, N (%)	7 (30.43%)	n.a
Treatment with DMT, N (%)	20 (86.96%)	n.a

treated with steroids in the month before the enrolment). At the time of tear collection, 5 patients (21.74%) were receiving moderate-efficacy disease-modifying treatments (DMTs), 15 patients (65.22%) were on high-efficacy DMTs, and 3 patients (13.04%) were untreated [32]. Exclusion criteria for tears collection in both RRMS patients and HCs were ocular diseases in the previous 12 months, history of topical therapy, and the use of contact lenses. Briefly, as reported by Rossi et al. [33], tears were collected on graduated Schirmer's strips asking the patients to look up and pulling the lower lid gently downward for 5 min and then extracted in 0.01 M PBS, Phosphate Buffered Saline (Sigma-Aldrich, St. Louis, MI, USA).

On the other hand, PB samples were used for protocol optimization and were obtained from 7 healthy Caucasian HCs who gave written informed consent. They did not declare themselves to be under chronic therapies, nor to be affected by chronic conditions.

Leukocyte-derived EVs staining and acquisition

To identify, phenotype and enumerate Leuko EVs, PB and tear samples, an already optimized and published flow cytometry protocol [34–37] adhering to all current ISEV flow cytometry guidelines, including MIFlowCyt-EV and MISEV2023 recommendation [38–40]. Briefly, samples were stained using 1 µL of LCD, 0.2 µL of fluorescein isothiocyanate (FITC)-conjugated phalloidin and 1 µL of CD45 Brilliant Violet 510 (BV510)-conjugated, all from BD Biosciences (San Jose, CA, USA). Samples were incubated at RT for 45 min in the dark and then diluted in PBS 1X before being filtered with 0.70 µm filter pore size. CD45+ events were acquired by flow cytometry (FACSVerse, BD Biosciences, San Jose, CA, USA) from RRMS and HC, as already reported [29]. Data were analysed using FACSDiva v 6.1.3 software (BD, BD Biosciences, San Jose, CA, USA). EV concentrations were obtained by volumetric count [29].

Leukocyte EVs purification by fluorescence-activated cell sorter

Tears and PB Leuko EVs were separated by instrumental cell sorting (100 µm nozzle, FACSAria III, BD Biosciences), based on the gating strategy shown in the scheme of Fig. 1, panels B–G. In detail, the trigger threshold was placed on the APC channel and, for all parameters, the height (H) signals, as well as bi-exponential or logarithmic modes were selected. The post-sorting purity was assessed by using the same instrument (FACSAria III) and the same setting applied for EVs separation, resulting anytime higher than 90% (not shown) [29, 30].

Nanoparticle tracking analysis

EVs isolated by FACS (350,000 EVs/sample) were analyzed using ZetaView (Particle Metrix GmbH, Meerbusch, Germany) equipped with a blue laser (488 nm, 40mW) and a long pass emission filter (LWP) for blue excitation laser (cut-off at 500 nm). The autofocus was adjusted to avoid indistinct particle visualization. Post-acquisition settings were optimized and maintained across sample analyses: for each sample 8–10 fields were analyzed, and a video of 30–60 s was recorded using ZetaView software. For each measurement a report for all analyzed parameters including mean, mode, and median size of EVs together with an estimation of concentration was obtained.

Atomic force microscopy

Atomic Force Microscopy (AFM) analysis was performed to investigate the size distribution and the morphology of the isolated total and Leuko EVs by using MultiMode 8 AFM microscope with Nanoscope V controller (Bruker, Billerica, Massachusetts, US). The samples were prepared by depositing a drop of diluted suspension of the isolated exosomes on SiO_2 wafer followed by drying in the oven at 37 °C for 2 h and then at room temperature overnight. The obtained samples were scanned by the silicon ScanAsyst-Air probe (triangular geometry, cantilever resonance frequency 70 kHz and nominal spring constant 0.4 N/m) in ScanAsyst in Air mode. Images of 512×512 pixels were collected with different scan sizes and were elaborated using NanoScope Analysis 1.8 software. The Particle Analysis tool of the software was used to detect and measure the size of the vesicles and the data were collected from the analysis of tens of particles captured from several AFM images.

Flow cytometry analysis of EV surface antigens

EV subtyping

Tears and PB EVs were identified, counted and subtyped using the panel detailed in Table S1. Briefly, 100 µL of tears or 5 µL of PB samples were stained using the reagent mix listed in Table S1. Samples were incubated for 45 min in the dark at RT, and diluted using 500 µl of PBS, as already reported [29].

EV marker detection

EVs were analyzed for the expression of CD63, and CD81, as detailed in Table S2. Samples were incubated for 45 min in the dark at RT, and then diluted using 500 µl of PBS.

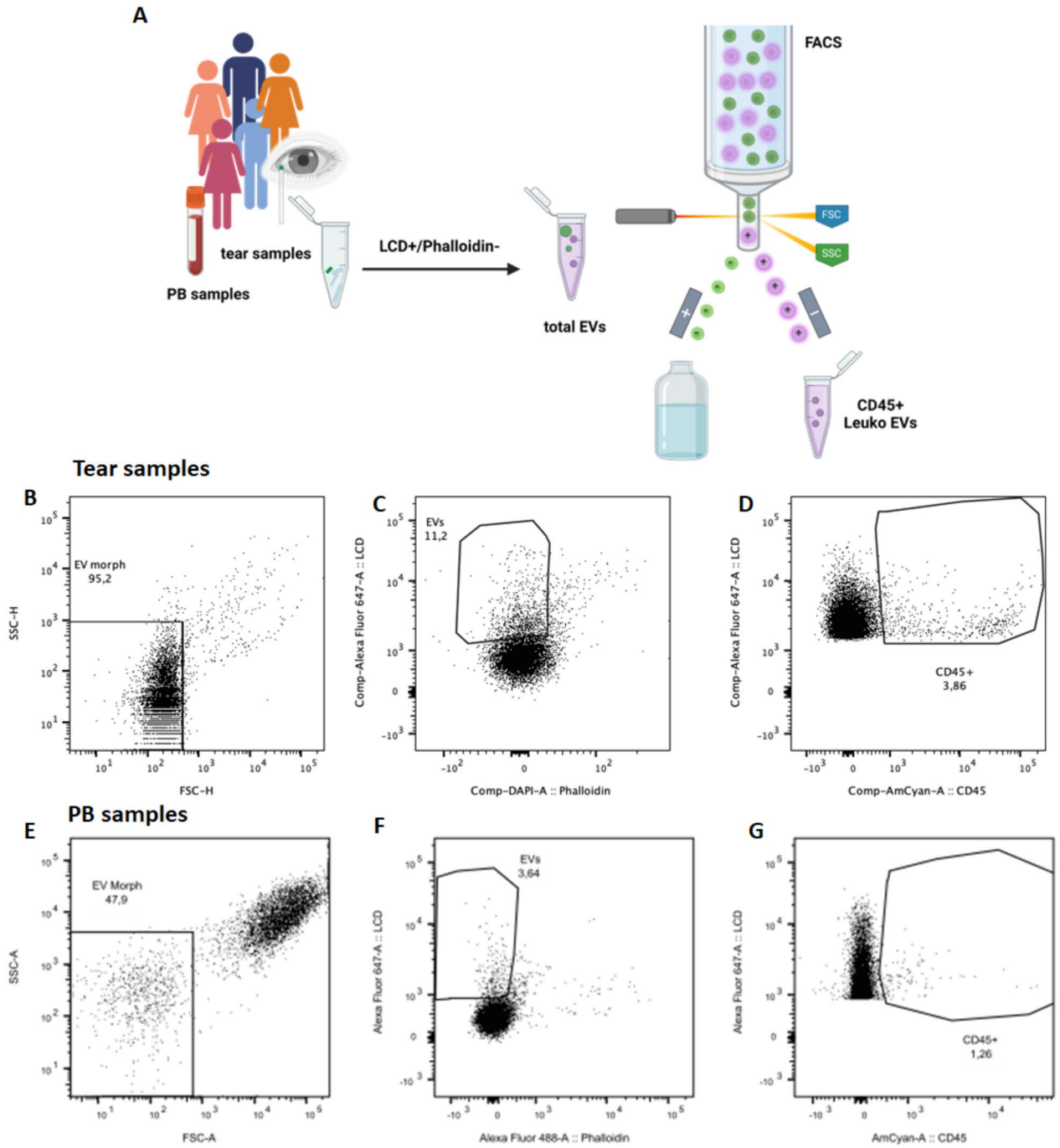

Fig. 1 Workflow, identification and isolation of tear and PB EVs. **A** EVs subtypes counts scheme in tears and PB samples of healthy subjects (HCs). The image was created by BioRender.com. **B** The scatter area containing EVs was firstly gated on FSC-H/SSC-H dot-plot; **C** Events positive to LCD (y-axis) and negativity to Phalloidin (x-axis) were identified as EVs; **D** EVs (LCD+/Phalloidin- events) were subtyped to identify leukocyte derived-EVs as events positive to CD45 (x-axis). **E**–**G** The same gating strategy was used to identify and separate PB EVs. Data are representative of all analysed samples

Flow cytometry EV acquisition

At least 1×10^6 EVs/sample were acquired using a CytoFLEX (Beckman Coulter, Sacramento, CA, USA) or a FACSVerse (BD Biosciences) flow cytometer, using a low (600–800) trigger threshold on the channel in which the LCD emits (APC channel) [37, 41]; CompBeads (BD Biosciences) and single stained samples were used to assess the compensation [42]. Fluorescence Minus One controls were used as recommended [34].

Leukocyte-derived EVs proteomics characterization

At first, we optimized the FACS-proteomics protocol on PB and tears EV samples for a single-phenotype characterization by sorting 2.0×10^6 (PB) and 1.4×10^5 (tears) of pooled CD45+ EVs from HCs. Meanwhile, in the second part of the study, the same number of Leuko-derived EVs (CD45+ EVs, 1.4×10^5) were sorted from tears of RRMS patients. As already published, the number of separated EVs was used as a normalization parameter for protein label-free identification and quantification [30]. In both cases, samples were prepared for FASP protocol by lysing Leuko EVs through sonication on ice (Sonicator U200S control, IKA Labortechnik, Staufen, Germany) at 70% amplitude in a lysis buffer (urea 6 M in 100 mM Tris/HCl, CHAPS 2% and Triton X-100 1% at pH = 7.5) using Amicon® Ultra Centrifugal Filters with 10 KDa molecular mass cut-off (MilliporeSigma Headqua, Massachusetts, USA). After that an overnight tryptic digestion was carried out at 37 °C in a buffer containing urea 8 M, Tris HCl 100 mM at pH = 8.5 on 10 KDa filters (Nanosep®, Membrana: Omega™, VWR International, Milan, Italy). EV tryptic peptides were analyzed in triplicate by nanoLC-MS/MS using the UltiMate™ 3000 UPLC (Thermo Fisher Scientific, Milan, Italy) chromatographic system coupled to the Orbitrap Fusion™ Tribrid™ (Thermo Fisher Scientific, Milan, Italy) mass spectrometer, as previously published in our works [36, 43]. Briefly, the flow rate was set at 300 nL/min, with a total run time of 65 min using a chromatographic gradient from 2 to 90% of phase B (phase A: water, phase B: acetonitrile, both with 0.1% formic acid). Orbitrap analyzer was used for MS1 scans with 240,000 of resolution and the signal intensity threshold at 1×10^4 for MS2 sequencing look at the ion trap performing a HCD fragmentation. Subsequently, MaxQuant, version 1.6.6.0, (Max-Planck Institute for Biochemistry, Martinsried, Germany) was used for processing raw MS/MS data with UniProt database (released 2020_06, taxonomy Homo Sapiens, 20,588 entries). All processing parameters and settings were reported in detail in our published works [36, 44]. Briefly, the false discovery rate (FDR) was set to 1% both for protein and for peptide levels. Match-between-runs (MBR) algorithm was used to transfer the peptide identifications from one LC–MS/MS run to all others using its default settings (match window of 0.7 min and alignment time of 20 min) [45]. Nonspecific cleavage to both ends of the peptides were allowed with maximum of 2 missed cleavages. In this regard, MS search output for protein quantification (i.e., number of peptides, proteins groups etc.) was detailed in raw file of Supplementary Table S9. For the second part of study and clinical application of FACS-Proteomics workflow, LFQ Intensity values were used for bioinformatics analyses performing by Perseus software, version 1.6.10.50, (Max-Planck Institute for Biochemistry, Martinsried, Germany) by fixing the minimum number of valid LFQ Intensity values at 2 in at least one clinical group (CV% was calculated between replicates to assess proteomics analysis variability showing a CV% < 50 for most of the quantified proteins, see Table S9) in order to evaluated not only the different protein modulation, but also the presence (fold change = 100) and absence (fold change = 0.01) of proteins between Leuko EV tears RRMS compared to HC ones. Subsequently, protein ratios (RRMS/HC) were used for functional enrichment analysis through "Core Analysis" of Ingenuity Pathway Analysis software (IPA, Qiagen, Hilden, Germany) [46]. The mass spectrometry proteomics data have been deposited to the ProteomeXchange Consortium via the PRIDE [47] partner repository with the dataset identifier PXD049036 and https://doi.org/10.6019/PXD049036.

Moreover, to define the differential proteins significantly expressed between pathologic group and control one, a univariate statistical analysis was performed with a p-value threshold of 0.05 visualizing results as Volcano Plot.

STRING version 12.0 (https://string-db.org/) analysis was used for evaluation of protein–protein interaction (PPI) networks and Gene Ontology (GO) enrichment analysis for cellular component (CC) together with Retrieve/ID mapping through UniProt SEARCH BOX [48].

FunRich (Functional Enrichment analysis tool, http://www.funrich.org/) version 3.1.4 release on 2020 was used to easily match our Leuko EV datasets with Vesiclepedia filtering the search to *Homo Sapiens* as species and using the whole deposited studies on biological fluids (e.g., blood, urine, saliva, plasma, serum, seminal fluids, amniotic fluids, aqueous humor and epididymal fluid) and vesicle types [49–51].

We have submitted all relevant data of our experiments to the EV-TRACK knowledgebase (EV-TRACK ID: EV240150) [52].

Results

Leukocyte-derived EVs identification, count and purification

In such a study, we focused on the analysis of CD45+ Leuko EVs single phenotype purification from biological fluids, given that they are particularly abundant both in tears and in PB.

Leuko EVs represent an EV subtype released from a quite heterogeneous population of immune cells, including granulocytes (neutrophils, eosinophils, and basophils), monocytes, and lymphocytes (T cells and B cells) recognised as CD45+ events. Thus, total and intact EVs of tear and PB samples were identified as LCD+/Phalloidin− events as reported in the gating strategies of Fig. 1 panels B–D (tears) and panels E–G (PB samples). As also endorsed by ISEV guidelines [11], CD45+ EVs events were reclassified as Leuko EVs (Fig. 1 panels D and G, respectively), detected and isolated by instrumental cell sorting, according to the reported gating strategy (Fig. 1). Moreover, such a population of EVs was purified from lacrimal fluids of patients affected by RRMS as described below. Therefore, we focused on the proteomics characterization of Leuko EVs purified from tears and PB samples.

The workflow shown in Fig. 2 summarizes the study design and the proteomics results highlighting both the samples and techniques used to characterize Leuko EV populations in terms of protein cargoes in the first optimizing phase of FACS-Proteomics method (tears and PB of HC) and in the second phase focusing on clinical application to RRMS tears.

Characterization of total and CD45+ EV features

Total EVs both from PB (Fig. 3A) and tears (Fig. 3B) of healthy volunteers were analysed by flow cytometry for the expression of CD63 and CD81 specific EV markers. As shown in Fig. 2, all the analysed EV populations displayed significant levels of tetraspanins, confirming their EV nature.

The isolated pure CD45+ EV fraction, both from tears and PB HC samples was characterized using Nanoparticle tracking analysis (NTA) and Atomic Force Microscopy (AFM). According to NTA, the whole population of EVs derived from PB or tear samples showed a median diameter of 120.3 nm and 105.4 nm respectively (Fig. 4A), while CD45+ EVs derived from PB or tear showed a median diameter of 127.5 nm and 145.8 nm, respectively (Fig. 4B). NTA results were in line with the size range detected by AFM for all EV samples. The AFM images of the 2D topography of total (Fig. 4A) and CD45+ EVs (Fig. 4B) revealed the presence of isolated vesicular structures characterized by different sizes. In line with NTA analysis results, pure total EV population sorted from PB and tears exhibited average diameters of 76.7 ± 29.6 nm and 109.3 ± 60.2 nm, respectively, while the mean particle sizes for Leuko-derived EVs isolated from blood and tears were 104.9 ± 50.9 nm and 82.7 ± 28.7 nm. The height profiles of representative EVs reported in Fig. 4 also confirmed the globular and flattened shape, likely due to the alteration induced by the drying step.

In this context, the NTA analysis showed that CD45+ EVs were characterized by an increased median diameter when compared to total EVs samples, significant only for EVs derived from tear samples (Table S3); on the other hand, AFM analysis highlighted statistical

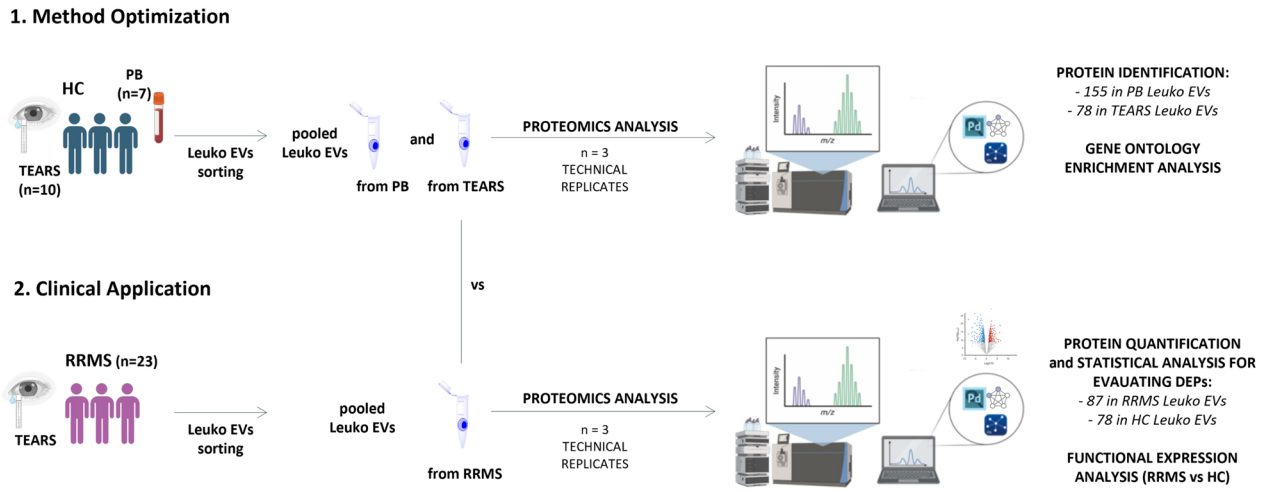

Fig. 2 Proteomics study workflow. PB: peripheral blood, Leuko EVs: leukocyte-derived EVs, HC: healthy controls, RRMS: relapsing–remitting multiple sclerosis, DEPs: differential expressed proteins. The image was created by BioRender.com

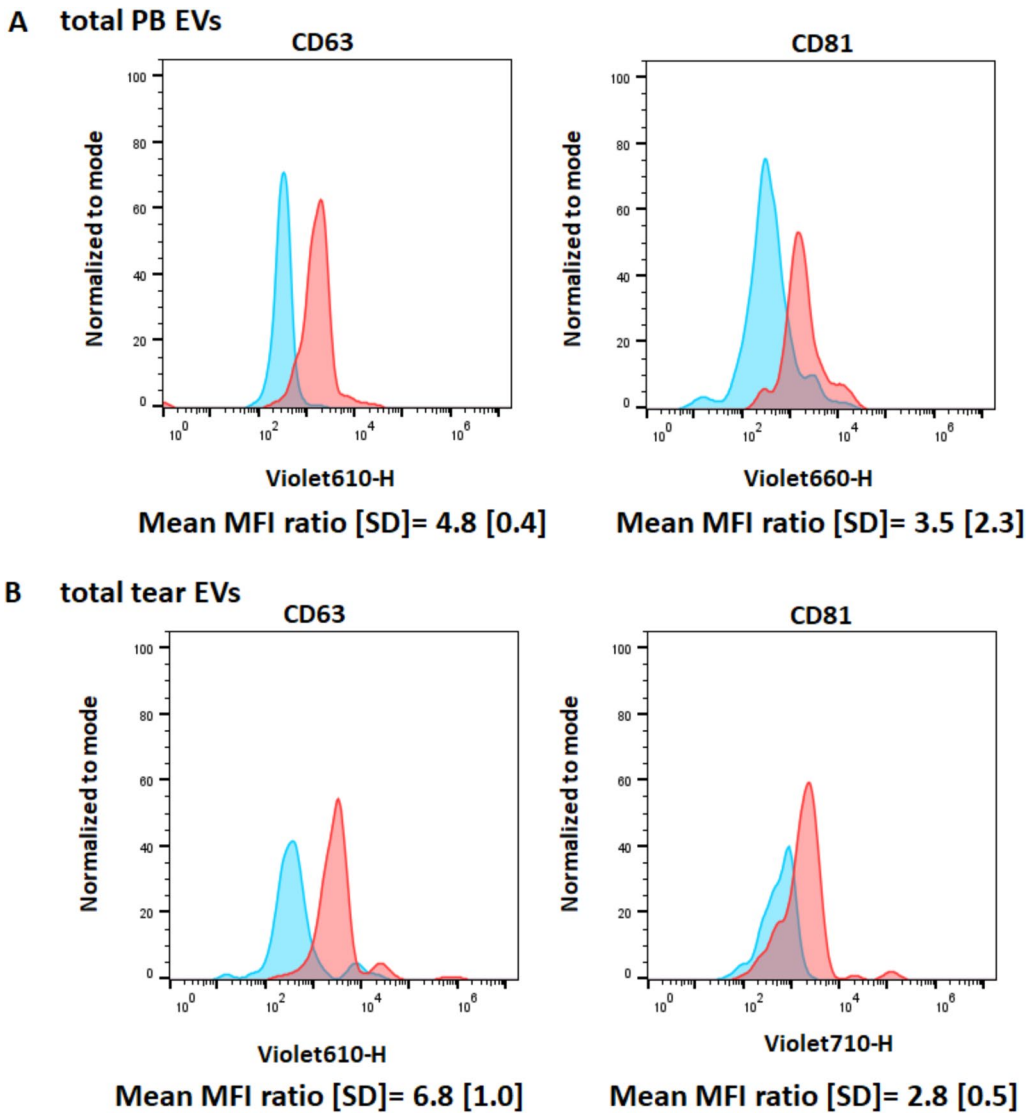

Fig. 3 Protein expression markers detection. Typical EV markers (CD63 and CD81) were analysed on the whole EV compartment both in PB (panel A) and in tear (panel B) samples

evidence only in the EVs samples derived from PB (Figure S1). Despite the slight discrepancy between AFM and NTA analyses, related to some variabilities between the two used techniques, the AFM measurements show a good level of agreement with NTA regarding the vesicles sizes, both of which are under 200 nm.

Detailed information about NTA measurements and results were listed in Supplementary Table S3.

Functional annotation of single-phenotype EVs proteomics in blood and tears

Purified Leuko EVs from pooled HC tears and PB were further analysed by proteomics. In detail, 1.4×10^5 and 2×10^6 events were purified as Leuko EVs from tears and PB, respectively, and, despite the limited amount of tear sample, we identified 78 proteins from tears Leuko EVs against 155 proteins form PB Leuko EVs. First, we compared the identified proteins to the reference EV platform Vesiclepedia (http://www.microvesicles.org) [49, 51], filtering the deposited studies on biological fluids, obtaining 88.67% and 92.31% of matching for Leuko EVs isolated from PB and from lacrimal Leuko EVs, respectively, as reported in Fig. 5A. All the identified proteins matched and unmatched in Vesiclepedia repository are reported in Supplementary Tables S5 and S6. Interestingly, going deep into the unmatched proteins, we found that they are mainly referred to as keratinocytes for tear fluid and immunoglobulins for PB, while about 90% of

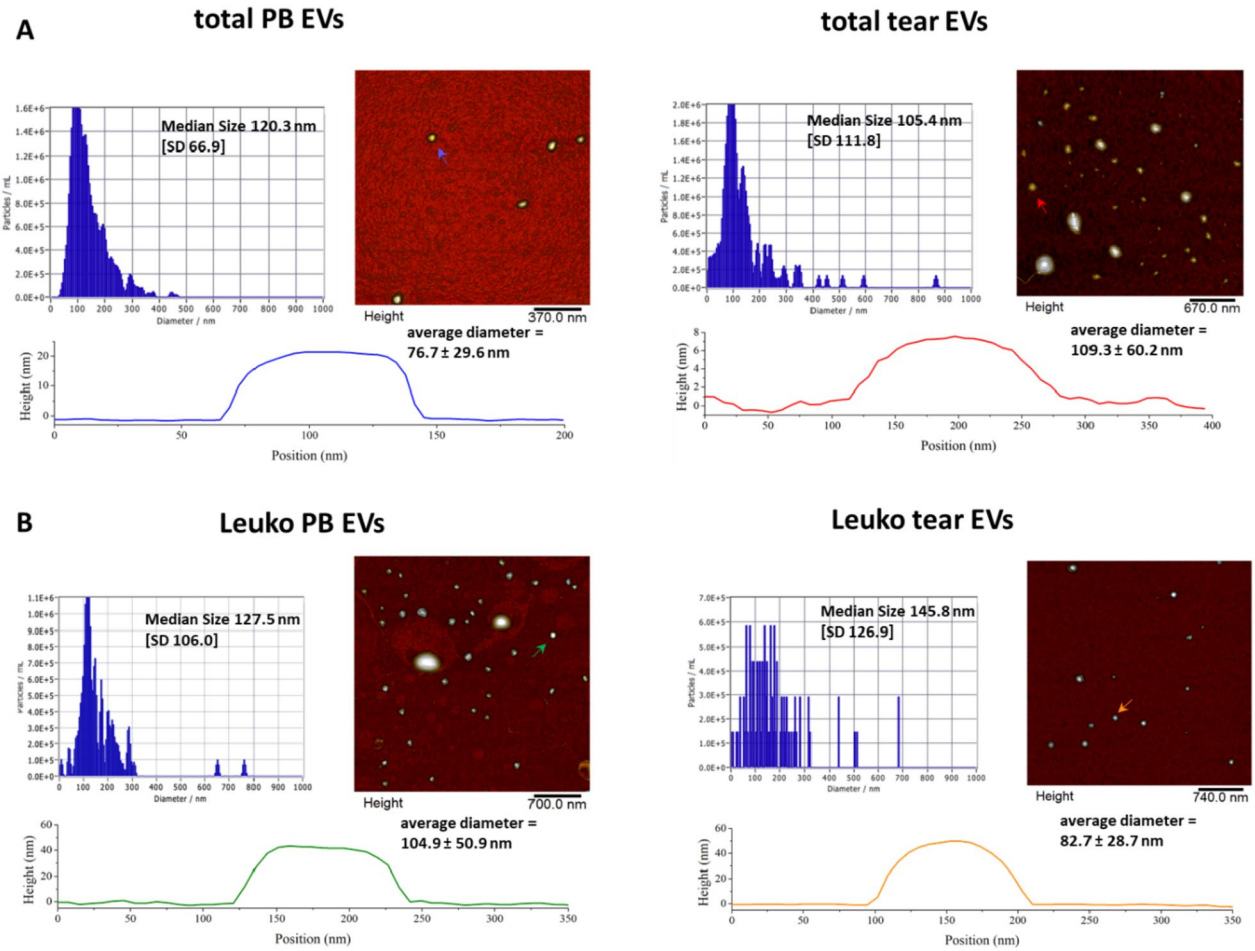

Fig. 4 Characterization of Leukocytes-derived EVs from healthy controls biofluids. **A** NTA tracking of size (diameter/nm) and concentration (particles/mL) of pure total EVs population sorted from PB (left) and tears (right). EVs derived from total PB or total tear showed a median diameter of 120.3 nm and 105.4 nm, respectively, falling within the size range detected by AFM reported in the figure. The height cross sectional profiles of representative vesicles of total PB (blue arrow) and total tear (red arrow) are also reported. **B** NTA tracking of size (diameter/nm) and concentration (particles/mL) of pure Leuko EVs sorted from PB (left) and tears (right). Leuko EVs derived from PB or tears showed a median diameter of 127.5 nm and 145.8 nm respectively, falling within the size range detected by AFM indicated in the figure. The height cross sectional profiles of representative Leuko EVs of PB samples (green arrow) and tears (orange arrow) are also reported

(See figure on next page.)

Fig. 5 Proteomics assessment of Leuko EVs sorted from PB and tears of healthy subjects. **A** Bar diagrams depict the matching between Leuko EV proteins and Vesiclepedia, an online EV proteome repository. Only 8.92% and 5.2% of the Leuko EV proteins were unmatched in Vesiclepedia for the pooled PB and tear samples, respectively. Details of all proteins are shown in Tables S5 and S6. **B** The Venn diagram shows the common proteins between PB Leuko EVs or tears Leuko EVs. **C**, **D** Gene Ontology (GO) classification of proteins are reported as red and blue dots to underline "extracellular exosome" and "vesicle" as the most significant cellular component in PB and lacrimal Leuko EVs with an FDR of 6.55×10^{-89} and 2.07×10^{-63} for PB Leuko EVs (**C**), and 1.23×10^{-35} and 2.22×10^{-30} for tears Leuko EVs (**D**), respectively. White dots represent proteins not identified with the GO classifications (see Table S7, sheets 4 and 5, for protein details). **E**, **F** Mechanistic networks of "leukocyte migration" downstream in PB Leuko EVs (p-value = 6.31×10^{-25}) and tears Leuko EVs (p-value = 5.95×10^{-8}). Shapes and symbols of proteins are shown in Figure S4

identified proteins are referred to the EV compartment. By comparing the identified proteins in Leuko EVs from both PB and tears, 17% of such proteins were found to be in common between the two biological fluids, as shown in the Venn diagram of Fig. 5B. Moreover, to study the Leuko EV protein cargoes from a functional point of

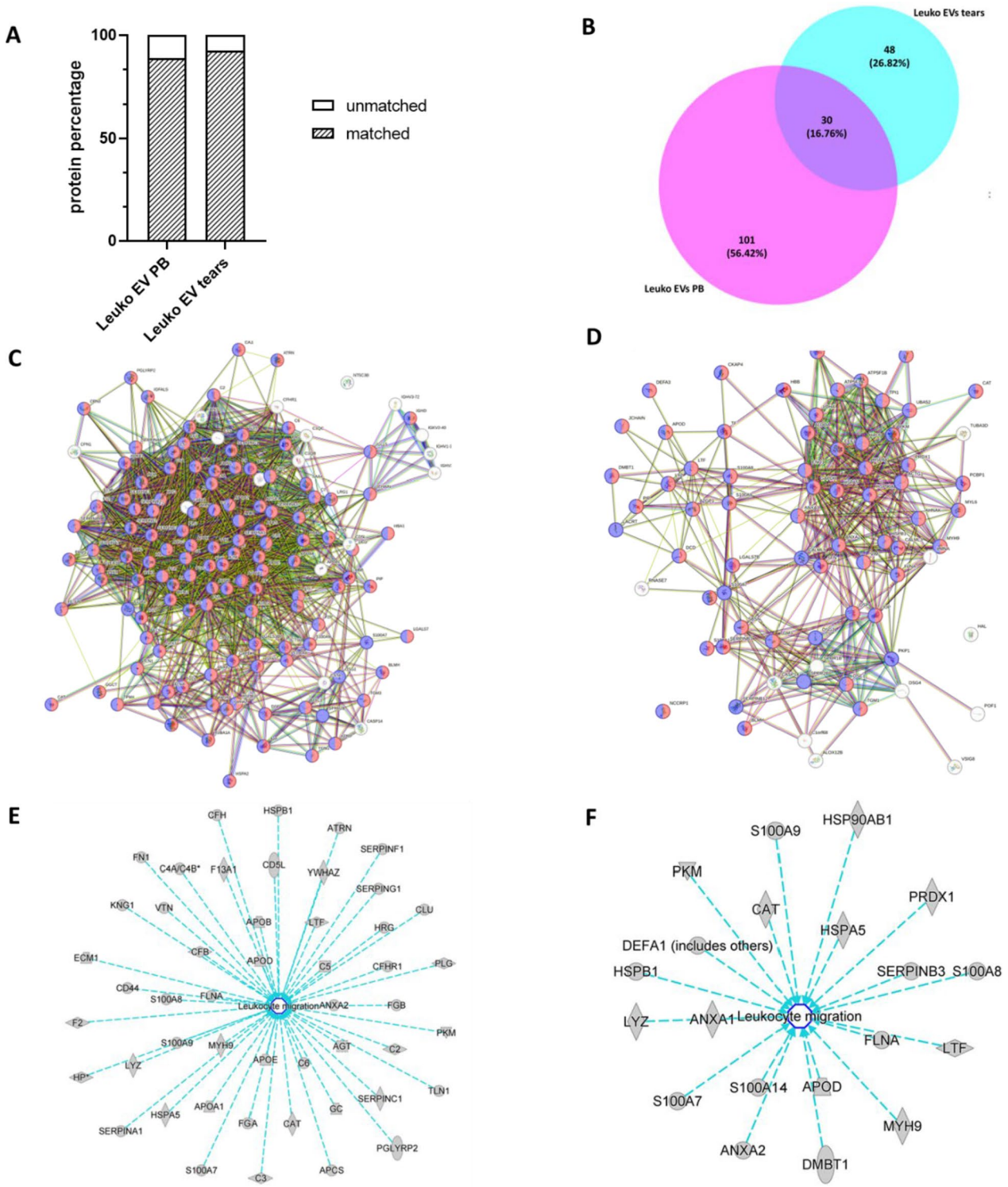

Fig. 5 (See legend on previous page.)

view, we performed a GO annotation processing of proteomics data to find putative network of interaction of the Leuko EV-enriched proteins identified in both biological fluids. They were analyzed for CC compartment showing that Leuko EVs proteomes have a strong enrichment of "Extracellular Exosome" (GO:0070062) associate proteins

(83.77% and 76.92% for PB and tears, respectively, as shown in Supplementary Table S7). Meanwhile, cytoplasmic proteins are poorly represented because only 6 (3.90%) and 8 (10.25%) proteins were uniquely reclassified as cytosolic proteins for PB and tear EV preparations, respectively (protein IDs highlighted in red in Table S7). Between them desmoglein-1 and protein S100-A7 were identified in common between Leuko EVs purified from two biological fluids. In this regard, we reported the interaction network of the identified proteins build by the STRING software in which the most significant cellular components referring to each protein have been highlighted by a color code for the proteins identified in Leuko EVs both from PB (panel C) and tears (panel D). In detail, the proteins that belong to the "Extracellular Exosome" (GO:0070062) component are highlighted in red with a FDR of 6.55×10^{-89} (for PB Leuko EVs) and FDR of 1.23×10^{-35} (for tears Leuko EVs), while the proteins that belong to the "vesicle" component (GO:0031982) are highlighted in blue with a FDR of 2.07×10^{-63} (for PB Leuko EVs) and 2.22×10^{-30} (for tear Leuko EVs), as reported in Fig. 5 panels C and D. White dots represent proteins not identified with the GO classifications. For the list of detail proteins see Supplementary Table S7, sheets 4 and 5. This phenotypic characterization corroborated simultaneously the isolation of intact EVs by instrumental cell sorting, as previously demonstrated in Marchisio et al. [29], and the EV sample preparation in term of purified proteins for proteomics purposes.

Going in deep to the leukocytes origin of sorted CD45+EVs, the same protein dataset was used for the expression analysis through IPA tool to predict the downstream effects associated to the protein expression found in Leuko EVs in the two analysed biological fluids. An overview of functional results is displayed in Table 3 depicting the main significant downstream effects expected by Leuko EV proteins from PB (on the left) and tears (on the right). In Fig. 5 we reported a mechanistic network of "leukocyte migration", resulting significantly covered by the protein dataset for PB Leuko EVs with an overlap p-value of 6.31×10^{-25} (panel E) and for tears Leuko EVs with a p-value of 5.95×10^{-8} (panel F). Notably, proteins involved in "leukocyte migration" in tear Leuko EVs overlapped to 23.2% of those in the PB demonstrating as in both body fluids the molecular information carried by Leuko EVs toward the recipient cells can be recognized and investigated. Among these, protein S100-A7, A8 and A9 were identified and connected each other because of their pro-inflammatory role and their contribution in leukocyte adhesion, migration and recruitment.

Among the significant downstream predicted by IPA software in Leuko EVs isolated from both biofluids, reported in Table 2, an overlap of 55.2% was observed. Moreover, most of the significant biological functions covered by the protein dataset in both biological fluids (reported in bold in Table 2) are associated to processes of immune system cells including granulocytes (neutrophils, basophils, and eosinophils) and mast cells. In addition to "leukocyte migration", we found also other downstream directly related to the origin cells, such as the "adhesion of neutrophils" (p-value $=1.08\times10^{-19}$ for PB Leuko EVs and 5.54×10^{-4} for tears Leuko EVs) and "cell movement of neutrophils" (p-value $=7.80\times10^{-18}$ for PB Leuko EVs and 4.12×10^{-5} for tears Leuko EVs).

We compared the GO terms and downstream observed in PB Leuko EVs to the total circulating EVs isolated from PB of the same pooled HC samples. Data were reported in Supplementary Table S4 and S7 and supported the specificity of the proteomics cargo obtainable by the isolation of a specific EVs phenotype.

For all functional GO analyses the complete list of downstream effects and the relative overlap p-values was reported in Table S8.

Leuko EVs protein expression in tears of multiple sclerosis

Our described FACS-proteomics approach was used to study Leuko EV protein cargo in tears from RRMS patients (n = 23) compared to HCs (n = 10). As preanalytics may change between HCs and patients, we assessed CD45+EVs purified from lacrimal fluids of RRMS subjects with NTA and AFM techniques showing a median diameter in line with those obtained by HC tears, as shown in Figure S2 and Table S3. Subsequently, 1.4×10^{5} Leuko EVs, isolated from pooled tears samples, underwent to proteomics analysis to explore their proteome cargo in RRMS patients compared to HCs. Protein numbers were consistent with those obtained in previous analyses [2, 30, 53]. Venn Diagram in Fig. 6A showed the summary of proteomics investigation in term of the common and unique proteins in the two analysed clinical conditions. 77.42% of proteins were in common between RRMS and HCs, while 22.58% of the proteins were identified and quantified only in Leuko EVs isolated from RRMS and/or HCs tears, as listed in Table 3. In particular, 15 proteins were quantified as unique proteins in RRMS Leuko EVs, and they showed significant interactions between them and were related to "Immune System HAS-168256 Reactome Pathway" (FDR $=2.07\times10^{-5}$, yellow dots) as demonstrated by STRING analysis (PPI enrichment p-value $=1.06\times10^{-6}$) and reported in Fig. 6B. Alongside these unique proteins, we compared the expression of common proteins between RRMS and HC Leuko EVs as reported in the Volcano plot of Fig. 6C highlighting 19 significantly up-regulated (red dots) and

Table 2 List of the main downstream effects predicted to be modulated by Leuko EVs protein from PB and tears of healthy subjects

DISEASE AND FUNCTIONS	PB	TEARS
Inflammation of organ	28.35	16.96
Leukocyte migration	24.20	7.23
Cell movement of leukocytes	20.48	7.22
Adhesion of neutrophils	18.97	3.26
Immune mediated inflammatory disease	18.69	15.18
Inflammation of absolute anatomical region	17.15	4.38
Cell movement of neutrophils	17.11	4.39
Cellular infiltration by leukocytes	16.85	3.80
Activation of leukocytes	15.45	N/A
Inflammation of joint	14.72	6.18
Infiltration by neutrophils	14.50	3.44
Cellular infiltration by granulocytes	13.98	N/A
Chronic inflammatory disorder	12.91	4.75
Immune response of cells	12.43	5.70
Migration of granulocytes	11.94	N/A
Cell movement of mononuclear leukocytes	10.09	N/A
Immune response of neutrophils	9.79	N/A
Migration of neutrophils	9.52	4.64
Aggregation of leukocytes	9.49	N/A
Cell movement of monocytes	8.16	N/A
Immune response of leukocytes	7.89	N/A
Activation of neutrophils	7.87	N/A
Migration of mononuclear leukocytes	7.83	N/A
Cell movement of granulocytes	18.36	5.38
Adhesion of immune cells	22.91	4.43
Accumulation of neutrophils	N/A	3.53
Accumulation of leukocytes	12.24	N/A
Accumulation of granulocytes	7.10	4.07
Chemoattraction of leukocytes	N/A	4.32

The expression functional data in term of -Log(p-value) and color is proportional to it are reported. The main significant biofunctions referred to EV phenotype (Leuko EVs) were highlighted in bold

(See figure on next page.)

Fig. 6 Clinical application of single phenotype EV proteomics workflow to tear fluid of Multiple Sclerosis patients. **A** Venn diagram of quantified proteins in Leuko EVs sorted from tears of RRMS patients and healthy volunteers. **B** Proteomics PPI assessment of RRMS unique proteins. Yellow dots were reclassified as proteins involved in "Immune System HAS-168256 Reactome Pathway". **C** Volcano Plot of proteins graphed by fold change (Difference) and -Log(p-value) by the comparison of RRMS vs HC subjects. Grey dots represent proteins that were not differentially expressed in the comparison carried out; red dots represent proteins that were significantly up-regulated and green dots indicate proteins that were significantly down-regulated in RRMS. **D** Regulator Effects network highlights the hypothesis of how "migration of endothelial cells" is activated by transforming growth factor beta 1 *(TGFB1)* as upstream regulator. **E** Networks of activated upstream regulators: Angiopoietin-2 *(ANGPT2)* and vascular endothelial growth factor group *(VEGF)*. **F** Downstream effect analysis reveals the upregulation of "angiogenesis". Orange and blue shapes represent predicted activation or inhibition, respectively. Instead, red and green shapes represent increased or decreased measurements of identified proteins, respectively, whose expression value is reported in the figure. Continuous lines represent direct relationships, dotted ones represent indirect relationships, whereas grey and yellow lines indicate the non-predicted and inconsistent relationships. Figure S4 reports an interpretation of IPA networks

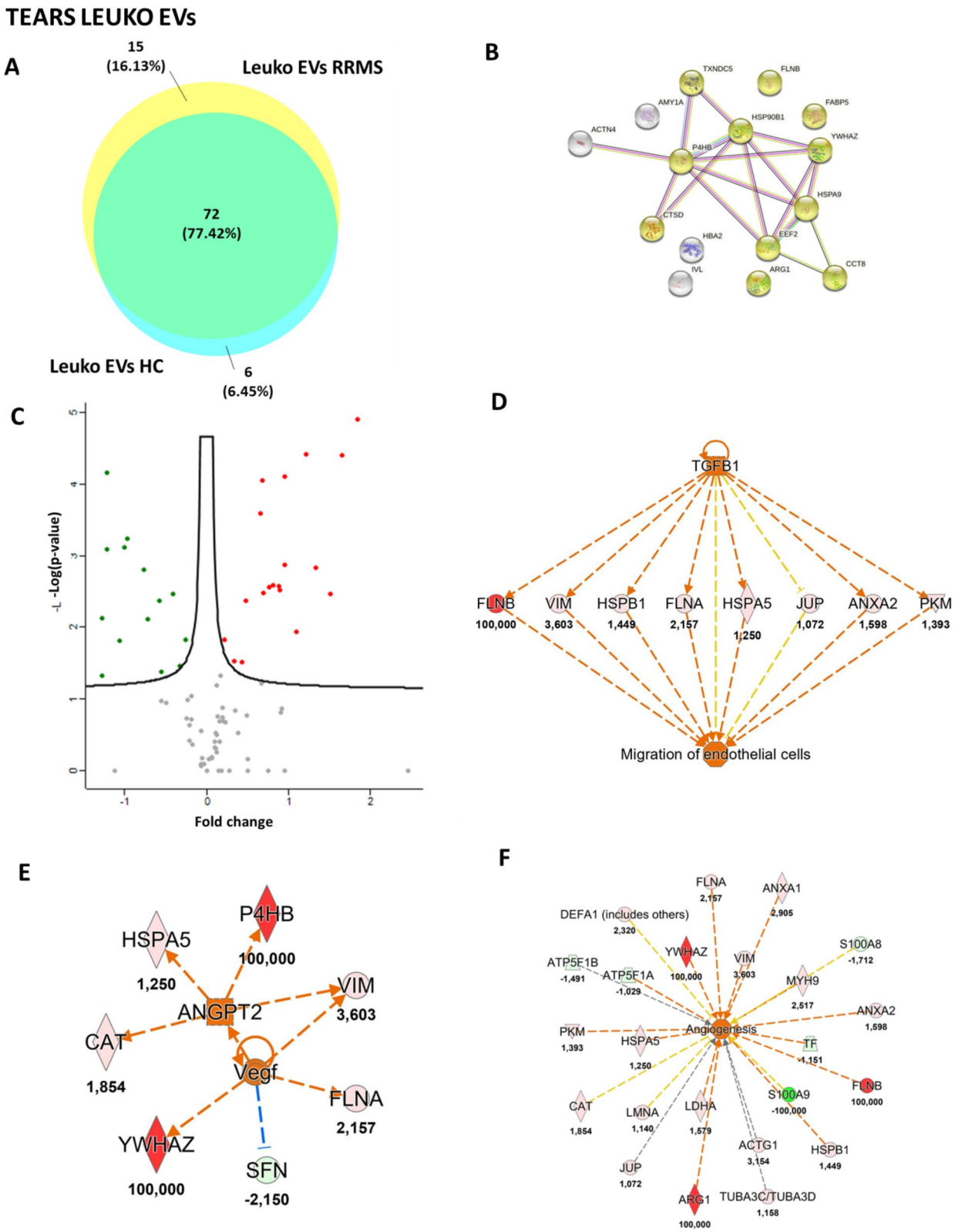

Fig. 6 (See legend on previous page.)

Table 3 Unique proteins identified in the Leuko EVs of two different clinical conditions (RRMS vs HC)

Gene name	Description	HC	RRMS
ALOX12B	Arachidonate 12-lipoxygenase, 12R-type	+	
S100A9	Protein S100-A9	+	
VSIG8	V-set and immunoglobulin domain containing 8	+	
LGALS7B	Lectin, galactoside-binding, soluble, 7B	+	
DSG4	Desmoglein-4	+	
RNASE7	Ribonuclease 7	+	
ACTN4	Alpha-actinin-4		+
FLNB	Filamin-B		+
ARG1	Arginase-1		+
P4HB	Protein disulfide-isomerase		+
CTSD	Cathepsin D		+
IVL	Involucrin		+
EEF2	Elongation factor 2		+
HSP90B1	Endoplasmin		+
HSPA9	Stress-70 protein, mitochondrial		+
CCT8	T-complex protein 1 subunit theta		+
YWHAZ	14-3-3 protein zeta/delta		+
HBA2	Hemoglobin subunit alpha 2		+
FABP5	Fatty acid-binding protein, epidermal		+
TXNDC5	Thioredoxin domain-containing protein 5		+
AMY1A	Alpha-amylase 1A		+

The sign "+" indicates the protein presence only in that clinical group

14 down-regulated (green dots) proteins in RRMS, as listed in Table 4.

LFQ Intensity values for each identified protein obtained through MaxQuant software were used as quantification parameter, and the LFQ ratio (RRMS/HC) was further employed as input for functional analysis by IPA tool. Figure 6D–F report the main proteomics functional results obtained by comparing the protein expression in the two-condition analysed. Tear Leuko EVs from RRMS patients have a protein expression able to trigger information related to a deep increase of neuroinflammation and angiogenic processes in RRMS patients.

Regulator Effects feature of IPA software can generate hypotheses about potential mechanisms that determinate the biological functions according to the related genes up- or down-regulated as well as upstream. In fact, network represented in Fig. 6D shows how "migration of endothelial cells" (p-value $= 7.08 \times 10^{-8}$, z-score = 2.00) function is significantly up-regulated via Leuko EVs proteins by *Transforming growth factor beta 1 (TGFB1)* (p-value $= 4.33 \times 10^{-8}$, z-score = 2.28) as activated upstream regulator in RRMS. This data corroborates the complex role of Leuko EVs as shuttles in the Immune System machinery in response to neuroinflammation and neurodegeneration scenario in RRMS. Moreover, endothelial cell migration is an essential event to trigger angiogenesis process, which is one of the most significant downstream in RRMS. Actually, Fig. 6 panel E indicates *Angiopoietin 2 (ANGPT2)* (p-value $= 1.17 \times 10^{-2}$) and *Vascular endothelial growth factor group (VEGF)* (p-value $= 1.62 \times 10^{-1}$) as significantly activated upstream regulators in RRMS Leuko EVs with z-scores of 2.00, involved in "vascular remodelling" and "angiogenesis" resulted deeply activated in RRMS Leuko EVs (p-value $= 2.87 \times 10^{-8}$, z-score = 1.92), as highlighted in the network of Fig. 6 panel F. The complete lists of downstream effects and upstream regulators for comparison RRMS vs HC were reported in Supplementary Table S8, sheets 3 and 4.

Discussion

In our previous reports we applied a new experimental workflow for isolating total EVs suitable for proteomics analysis, directly from untouched body fluids [2, 8, 30, 53, 54]. The method was applied for isolating and studying the total EV population in different pathological context and took advantage of an optimized FACS sorting isolation protocol coupled to mass spectrometry-based proteomics characterization [2, 8, 30, 33]. However, the study of ex-vivo cell-specific EV subsets should be considered the main target in this setting but, at the same time, represents an ongoing challenge [55]. EVs from cell cultures are a good way to access at single EV phenotypes, however, scientific results obtainable couldn't represent the picture of the in vivo real EV behaviour, especially because of the EV mediated intercellular crosstalk complex machineries and should be taken with caution. Here, we reported an update on the EV characterization, by exploiting, for the first time, the intrinsic purification capability of FACS sorting based on labelled-recognition events and focusing on the isolation and proteomics characterization of a specific sub-type of circulating EVs. The first single EV phenotype proteomics application was carried out on Leuko EVs from PB and tears of enrolled volunteers by sorting CD45+ EVs. We are aware about the heterogeneity of such a population released from different immune cell types and the reason of the Leuko EVs sub-type choice arose from the need of a large population as possible due to the extremely low amount of material for proteomics analysis and then for our interest in a deeply characterization of the EV-mediated immune system machinery in RRMS [56]. Based on our previously published results in which we demonstrated the purity and the size distribution of isolated EVs [29], we were quite confident about the efficiency of the FACS sorting protocol in term of purity and quality of the sorted Leuko EV samples, after confirmed by the obtained proteomics

Table 4 Differential proteins in Leuko EVs isolated from tears of RRMS patients compared to HCs

Expression in RRMS	Gene names	Description	−Log(p-value)	Difference
Down	*GGCT*	Gamma-glutamylcyclotransferase	1.83	−0.26
Up	*LDHA*	L-lactate dehydrogenase A chain	3.59	0.66
Down	*LTF*	Lactotransferrin	3.11	−1.00
Up	*CAT*	Catalase	2.52	0.89
Up	*ALDOA*	Fructose-bisphosphate aldolase A	1.53	0.34
Up	*ANXA1*	Annexin A1	2.46	1.50
Down	*S100A8*	Protein S100-A8	2.81	−0.77
Up	*ANXA2*	Annexin A2	4.05	0.67
Up	*HSP90AB1*	Heat shock protein HSP 90-beta	2.56	0.76
Up	*VIM*	Vimentin	4.90	1.85
Up	*UBA52*	Ubiquitin-60S ribosomal protein L40	2.87	0.95
Up	*PKM*	Pyruvate kinase PKM	2.37	0.48
Up	*FLNA*	Filamin-A	1.93	1.10
Down	*SPRR2A*	Small proline-rich protein 2A	2.11	−0.72
Down	*CALML3*	Calmodulin-like protein 3	2.12	−1.28
Down	*SERPINB3*	Serpin B3	2.37	−0.58
Down	*S100A7*	Protein S100-A7	3.23	−0.96
Down	*SFN*	14-3-3 protein sigma	1.81	−1.06
Up	*MYH9*	Myosin-9	2.83	1.33
Up	*DEFA3*	Neutrophil defensin 3	4.42	1.21
Up	*ACTG1*	Actin, cytoplasmic 2	4.40	1.66
Down	*HIST1H4A*	Histone H4	4.16	−1.22
Up	*HBB*	Hemoglobin subunit beta	4.11	0.96
Up	*DCD*	Dermcidin	1.52	0.42
Up	*PRDX1*	Peroxiredoxin-1	2.59	0.81
Down	*TGM3*	Protein-glutamine gamma-glutamyltransferase E	2.46	−0.41
Up	*DSC1*	Desmocollin-1	2.48	0.69
Down	*PKP1*	Plakophilin-1	1.47	−0.33
Down	*BLMH*	Bleomycin hydrolase	1.33	−1.27
Up	*SBSN*	Suprabasin	2.57	0.88
Up	*SERPINB12*	Serpin B12	1.82	0.22
Down	*LACRT*	Extracellular glycoprotein lacritin	1.38	−0.55
Down	*DMBT1*	Deleted in malignant brain tumors 1 protein	3.09	−1.22

Leuko EV proteins significantly up- and down-regulated in pooled RRMS tears are indicated by red and green dots in the Volcano Plot, respectively, according to p-value and "Difference" values reported in the table

results. Actually, Leuko EVs in PB and tears were identified as LCD+/Phalloidin-/CD45+ events, isolated by fluorescence-activated cell sorting and characterized by AFM and NTA, revealing an EV mean diameter < 200 nm (small EVs according to MISEV 2023 classification). The post-sorting purity was assessed by using the same setting applied for EVs separation, resulting anytime higher than 90% (not shown). Based on our knowledge, this is the first time that Leuko EVs were recognized and isolated from PB and lacrimal fluid of the same volunteers paving the way to single-phenotype EV characterization from biological fluids. Proteomics results demonstrated a coded protein cargo of Leuko EVs found in the lacrimal fluid reflecting that observed in PB, opening the door to a major investigation perspective in the study of EVs from tears. Likely due to the major number of events sorted in PB, we found a greater number of identified proteins in PB Leuko EVs than those identified in tears Leuko EVs. Despite this discrepancy in numbers, a similar protein cargo conveyed in tears and PB Leuko EVs was found, which fits into a context of common leukocytes biological functions. Moreover, we identified a specific significant cluster of 20 proteins in lacrimal Leuko EVs associated to "RNA binding" function, indicating as Leuko EV information about RNA loading conveyed into target cells can be better recognised in tears [57, 58] (the same function

in PB was not significant and referring to 7 of the 20 proteins found in tears, see Table S7, sheets 4 and 5).

Moreover, as a proof of concept, among the cellular functions significantly described by both protein cargoes there was *"leukocyte migration"*, demonstrating how the here proposed FACS-Proteomics approach is highly selective in isolating and characterizing the protein cargo of circulating Leuko EVs from blood and even from lacrimal fluid (see Table S4 where many biofunctions related to Leuko EVs biogenesis were listed for total PB EV protein dataset showing less significant p-values than PB Leuko EV proteins).

As a main aspect of these results there is the opportunity to consider the lacrimal fluid EVs as a container of extractable biological information for improving molecular mechanisms knowledge and discover novel biomarkers and therapeutics targets across a wide range of pathological conditions especially looking at central nervous system affecting diseases. Previously, we determined tear total EVs protein cargo in RRMS subjects highlighting a pathological protein profile in EVs that likely referred to immune cell activation [30]. Here, we carried out the first EVs single-phenotype proteomics investigation in RRMS through a label free proteomics approach on Leuko EVs purified from tears of RRMS patients. Proteomics results demonstrated as Leuko EVs in RRMS are enriched with a specific protein cargo reflecting the activation of many factors like *TGFB1* as main upstream in the parental cells that exploits EVs to spread out their biological information through proteins messengers of inflammation and angiogenesis processes as main downstream predicted by bioinformatics analysis. According to IPA prediction and hypothesis, its overexpression could determine an increase of the "migration of endothelial cells". Blood–brain-barrier (BBB) is composed of cerebral endothelial cells, which have a central role in trans-BBB leukocyte diapedesis during normal immune surveillance as well as neuroinflammatory conditions like RRMS [59, 60], where the integrity of BBB is impaired [61]. Our data demonstrated that protein cargo of lacrimal Leuko EVs reflects on the one hand the neuroinflammatory condition of RRMS (*TGFB1* and *NFE2L2*, upstream regulators activated) and on the other hand endothelial cell proliferation together with an increase of vascular networks (*AGNPT2* and *Vegf*, upstream regulators activated) during RRMS due to pro-angiogenic processes. In this regard, new vessel formation has been studied in many pathological conditions including RRMS and in its animal model (i.e., EAE, experimental allergic encephalomyelitis) [62, 63]. This phenomenon is directly connected to leukocyte infiltration through the BBB and its increased permeability is driven by *VEGF* that regulates vessel growth and, in the meantime, has chemotactic functions against lymphocytes and monocytes, promoting neuroinflammation. Together with Vegf, another important regulated upstream gene resulted activated by a set of RRMS Leuko EV proteins is *ANGPT2*, which was found increased in neurons, glia and inflammatory cells during EAE [64]. In agreement with these results, we revealed an activation of angiogenesis function which have been highlighted as up-regulated downstream effects also in PI3K/AKT signaling pathway (p-value $= 6.93 \times 10^{-3}$, z-score = 2.00, Figure S3).

These functional proteomics results seem to be quite similar to those obtained by proteomics investigations on total EVs sorted from tears in RRMS subjects [30], unveiling that most of proteomics data in the analysis of total tears EVs come from circulating Leuko EVs, likely due to the immune system involvement in RRMS, besides the fact that they are one of the most abundant populations of EV phenotypes in tears, influencing the total protein expression.

Here, we provided a proof of concept and a perspective on the potential and challenges of the FACS-Proteomics isolation/characterization of single EV subtypes that can be further characterized from whole biological fluids without any kind of pre-analytical manipulation step, emphasizing the use of tears, collected using the Shirmer's strip kit usually adopted in ophthalmology routine, which have proved to be a precious source of biological information not only in ocular pathologies [26]. Of note, proteomics results could be affected (especially in blood) from the formation of protein corona that forms spontaneously around many, if not all, nanoparticles in biological fluids [65]. Due to their importance as an in vivo address code on the EV surface specificity [66], this aspect will be considered in a more focused and future investigation. Actually, the peculiar EV isolation approach and the different matrix microenvironment of different biological fluids may result in different proteins being identified as potential EV corona proteins. However, the question if these proteins were contaminants or inherent components of EVs is still open. Due to the limited number of proteins obtainable from a single tear sample, quantitative proteomics data were carried out by pooling specimens. It is also noteworthy that a larger number of purified EVs should establish deeper and more complete proteomic coverage of CD45+ EVs from tears, but this would require pooling many more samples. In fact, pooling patient samples is the main limitation of our exploratory study, as it may not accurately reflect the EV proteins pattern of individual subjects. Moreover, we believe that the pooled samples were more representative of the majority that are taking high-efficacy DMTs. Therefore, to better investigate the role of Leuko EVs in such a multifactorial and autoimmune disease, the

identified modulated inflammatory pathways could be further and deeply validated in a cohort of independent RRMS patients, taking into account not only the clinical outcomes but also the different treatments.

However, the rapid progress in mass spectrometry technologies and PFC tools promises to push the limits towards on single biological sample and to enable up to many orders of magnitude increased throughput in the proteomics characterization even of less abundant circulating EVs phenotypes, giving us the opportunity to improve our knowledge of real EVs behaviour in vivo.

In this context, the potential of mass spectrometry to provide sensitive identification of biomarkers in single-phenotype EVs, as shown in this study for Leuko EVs, could be integrated and supported by other high-throughput techniques, such as quantitative polymerase chain reaction (qPCR), to ensure the accuracy and reliability of the identified protein expression profiles for each individual clinical patient profile towards EV clinical applications and personalized medicine.

Abbreviations

AFM	Atomic force microscopy
APC	Allophycocyanin
CC	Cellular component
CSF	Cerebrospinal fluid
DDA	Data dependent acquisition
DMTs	Disease-modifying treatments
EVs	Extracellular Vesicles
FACS	Fluorescent-activated cell sorting
FASP	Filter-assisted sample preparation
FDR	False discovery rate
FITC	Fluorescein isothiocyanate
GO	Gene Ontology
HC	Healthy controls
IPA	Ingenuity Pathway Analysis
LCD	Lipophilic cation dye
LC–MS/MS	Liquid chromatography tandem mass spectrometry
Leuko EVs	Leukocyte-derived EVs
LFQ	Label-free quantification
NTA	Nanoparticle tracking analysis
PB	Peripheral blood
PFC	Polychromatic flow cytometry
PPIs	Protein–protein interactions
RRMS	Relapsing–remitting multiple sclerosis

Supplementary Information

The online version contains supplementary material available at https://doi.org/10.1186/s12967-025-06558-4.

Supplementary material 1 Table S1: Flow cytometry reagent list for EV marker detection; Table S2: Flow cytometry reagent list for EV marker detection; Table S3: NTA acquisition details. Table S4: List of the main downstream effects predicted to be modulated by total and Leuko EVs protein from PB of healthy subjects; Table S5: Leuko EV proteins identified in PB and tears of healthy volunteers matched in Vesiclepedia database; Table S6: Leuko EV proteins unmatched in Vesiclepedia database; Table S7: Gene Ontology (GO) annotation for cellular component (CC); Table S8: List of downstream effects and upstream regulators predicted by IPA software; Table S9: MS search output for Leuko EV protein quantification in RRMS and HC tears; Figure S1: Evaluation of EVs diameters obtained with AFM measurements; Figure S2: Characterization of Leukocytes-derived EVs from RRMS patients; Figure S3: Activation of Phosphoinositide 3-OH kinase (PI3K)/AKT Signaling pathway; Figure S4: IPA legend interpretation.

Author contributions

Conceptualization: P.D.B, P.L., M.C.C. and. D.P.; formal analysis: M.C.C., D.D.B., A.D.S., S.V., A.P., D.B., P.S. and S.P.; funding acquisition: P.D.B.; data curation: A.F., S.V., D.B., D.P., I.C. and M.C.C.; investigation: V.T. and M.G.R.; methodology: M.C.C, I.C., P.S. and P.L.; project administration, validation and visualization: P.D.B.; resources and supervision: P.D.B., P.L. and D.P.; writing original draft: M.C.C., I.C., P.L. and P.D.B.; and writing-review and editing: L.F., R.M.H.K., V.T. and A.F. All authors have read and agreed to the published version of the manuscript.

Funding

A.F and S.P. thank European Union – NextGenerationEU under the National Recovery and Resilience Plan (NRRP), Mission 4 Component 2—M4C2 Investiment 1.5 - Call for tender No. 3277 of DATE 30 dicembre 2021 Italian Ministry of University, Award Number: ECS00000041, Project Title: "Innovation, digitalisation and sustainability for the diffused economy in Central Italy", Concession Degree No. 1057 of DATE 23.06.2022 adopted by the Italian Ministry of University CUP: D73C22000840006 - Title of the project: Vitality: One-Health telemedicine and environment, WP 4: Precision medicine for cell/tissue therapy and pollution contrast, for funding this study.

Availability of data and materials

The mass spectrometry proteomics data have been deposited to the ProteomeXchange Consortium via the PRIDE partner repository with the identifier PXD049036. We have submitted all relevant data of our experiments to the EV-TRACK knowledgebase (EV-TRACK ID: EV240150).

Declarations

Ethics approval and consent to participate

The protocol was approved on 29 December 2020 by the Ethic committee of "G. d'Annunzio".

Consent for publication

Not applicable.

Informed consent

Informed consent was obtained from all subjects involved in the study.

Competing interests

Not applicable.

Author details

[1]Department of Innovative Technologies in Medicine and Dentistry, G. d'Annunzio University of Chieti-Pescara, 66100 Chieti, Italy. [2]Center for Advanced Studies and Technology (CAST), G. d'Annunzio University of Chieti-Pescara, 66100 Chieti, Italy. [3]Department of Medicine and Aging Sciences, G. d'Annunzio University of Chieti-Pescara, 66100 Chieti, Italy. [4]Department of Pharmacy, G. d'Annunzio University of Chieti-Pescara, 66100 Chieti, Italy. [5]Department of Science, G. d'Annunzio University of Chieti-Pescara, 66100 Chieti, Italy. [6]Department of Medical, Oral and Biotechnological Sciences, G. d'Annunzio University of Chieti-Pescara, 66100 Chieti, Italy. [7]Department of Neurobiology Research, Institute of Molecular Medicine, University of Southern Denmark, 5000 Odense, Denmark. [8]Department of Neurosciences, Imaging, and Clinical Sciences, "G. d'Annunzio" University, Chieti-Pescara, Italy.

Received: 30 January 2025 Accepted: 30 April 2025
Published online: 20 May 2025

References

1. Krämer-Albers E-M, Werner HB. Mechanisms of axonal support by oligodendrocyte-derived extracellular vesicles. Nat Rev Neurosci. 2023;24:474–86.

2. Brocco D, Lanuti P, Pieragostino D, Cufaro MC, Simeone P, Bologna G, et al. Phenotypic and proteomic analysis identifies hallmarks of blood circulating extracellular vesicles in NSCLC responders to immune checkpoint inhibitors. Cancers. 2021;13:585.
3. Wang G, Li J, Bojmar L, Chen H, Li Z, Tobias GC, et al. Tumour extracellular vesicles and particles induce liver metabolic dysfunction. Nature. 2023;618:374–82.
4. Simeone P, Bologna G, Lanuti P, Pierdomenico L, Guagnano MT, Pieragostino D, et al. Extracellular vesicles as signaling mediators and disease biomarkers across biological barriers. Int J Mol Sci. 2020;21:2514.
5. van Niel G, D'Angelo G, Raposo G. Shedding light on the cell biology of extracellular vesicles. Nat Rev Mol Cell Biol. 2018;19:213–28.
6. Samuel M, Fonseka P, Sanwlani R, Gangoda L, Chee SH, Keerthikumar S, et al. Oral administration of bovine milk-derived extracellular vesicles induces senescence in the primary tumor but accelerates cancer metastasis. Nat Commun. 2021;12:3950.
7. Pieragostino D, Lanzini M, Cicalini I, Cufaro MC, Damiani V, Mastropasqua L, et al. Tear proteomics reveals the molecular basis of the efficacy of human recombinant nerve growth factor treatment for neurotrophic keratopathy. Sci Rep. 2022;12:1229.
8. Falasca K, Lanuti P, Ucciferri C, Pieragostino D, Cufaro MC, Bologna G, et al. Circulating extracellular vesicles as new inflammation marker in HIV infection. AIDS. 2021;35:595–604.
9. Single-cell proteomics: challenges and prospects. Nat Methods. 2023;20:317–8.
10. Morales-Sanfrutos J, Munoz J. Unraveling the complexity of the extracellular vesicle landscape with advanced proteomics. Expert Rev Proteomics. 2022;19:89–101.
11. Welsh JA, Goberdhan DCI, O'Driscoll L, Buzas EI, Blenkiron C, Bussolati B, et al. Minimal information for studies of extracellular vesicles (MISEV2023): from basic to advanced approaches. J Extracell Vesicles. 2024;13: e12404.
12. Choi D, Rak J, Gho YS. Isolation of extracellular vesicles for proteomic profiling. Methods Mol Biol. 2021;2261:193–206.
13. Brady JV, Troyer RM, Ramsey SA, Leeper H, Yang L, Maier CS, et al. A preliminary proteomic investigation of circulating exosomes and discovery of biomarkers associated with the progression of osteosarcoma in a clinical model of spontaneous disease. Transl Oncol. 2018;11:1137–46.
14. Niu Z, Pang RTK, Liu W, Li Q, Cheng R, Yeung WSB. Polymer-based precipitation preserves biological activities of extracellular vesicles from an endometrial cell line. PLoS ONE. 2017;12: e0186534.
15. Gámez-Valero A, Monguió-Tortajada M, Carreras-Planella L, la Franquesa M, Beyer K, Borràs FE. Size-exclusion chromatography-based isolation minimally alters extracellular Vesicles' characteristics compared to precipitating agents. Sci Rep. 2016;6:33641.
16. Sun Y, Huo C, Qiao Z, Shang Z, Uzzaman A, Liu S, et al. Comparative proteomic analysis of exosomes and microvesicles in human saliva for lung cancer. J Proteome Res. 2018;17:1101–7.
17. Kanwar SS, Dunlay CJ, Simeone DM, Nagrath S. Microfluidic device (ExoChip) for on-chip isolation, quantification and characterization of circulating exosomes. Lab Chip. 2014;14:1891–900.
18. Wang Z, Wu HJ, Fine D, Schmulen J, Hu Y, Godin B, et al. Ciliated micropillars for the microfluidic-based isolation of nanoscale lipid vesicles. Lab Chip. 2013;13:2879–82.
19. Marassi V, Maggio S, Battistelli M, Stocchi V, Zattoni A, Reschiglian P, et al. An ultracentrifugation - hollow-fiber flow field-flow fractionation orthogonal approach for the purification and mapping of extracellular vesicle subtypes. J Chromatogr A. 2021;1638: 461861.
20. Zhang Q, Jeppesen DK, Higginbotham JN, Franklin JL, Coffey RJ. Comprehensive isolation of extracellular vesicles and nanoparticles. Nat Protoc. 2023;18:1462–87.
21. MacCoss MJ, Alfaro JA, Faivre DA, Wu CC, Wanunu M, Slavov N. Sampling the proteome by emerging single-molecule and mass spectrometry methods. Nat Methods. 2023;20:339–46.
22. Selmaj I, Mycko MP, Raine CS, Selmaj KW. The role of exosomes in CNS inflammation and their involvement in multiple sclerosis. J Neuroimmunol. 2017;306:1–10.
23. Teekaput C, Thiankhaw K, Chattipakorn N, Chattipakorn SC. Possible roles of extracellular vesicles in the pathogenesis and interventions of immune-mediated central demyelinating diseases. Exp Neurobiol. 2024;33:47–67.
24. Geraci F, Ragonese P, Barreca MM, Aliotta E, Mazzola MA, Realmuto S, et al. Differences in intercellular communication during clinical relapse and gadolinium-enhanced MRI in patients with relapsing remitting multiple sclerosis: a study of the composition of extracellular vesicles in cerebrospinal fluid. Front Cell Neurosci. 2018. https://doi.org/10.3389/fncel.2018.00418.
25. Agliardi C, Guerini FR, Zanzottera M, Bolognesi E, Picciolini S, Caputo D, et al. Myelin basic protein in oligodendrocyte-derived extracellular vesicles as a diagnostic and prognostic biomarker in multiple sclerosis: a pilot study. Int J Mol Sci. 2023;24:894.
26. Pieragostino D, Cicalini I, Lanuti P, Ercolino E, di Ioia M, Zucchelli M, et al. Enhanced release of acid sphingomyelinase-enriched exosomes generates a lipidomics signature in CSF of multiple sclerosis patients. Sci Rep. 2018;8:3071.
27. Welton JL, Loveless S, Stone T, von Ruhland C, Robertson NP, Clayton A. Cerebrospinal fluid extracellular vesicle enrichment for protein biomarker discovery in neurological disease; multiple sclerosis. J Extracell Vesicles. 2017. https://doi.org/10.1080/20013078.2017.1369805.
28. D'Anca M, Fenoglio C, Buccellato FR, Visconte C, Galimberti D, Scarpini E. Extracellular vesicles in multiple sclerosis: role in the pathogenesis and potential usefulness as biomarkers and therapeutic tools. Cells. 2021;10:1733.
29. Marchisio M, Simeone P, Bologna G, Ercolino E, Pierdomenico L, Pieragostino D, et al. Flow cytometry analysis of circulating extracellular vesicle subtypes from fresh peripheral blood samples. Int J Mol Sci. 2020;22:48.
30. Pieragostino D, Lanuti P, Cicalini I, Cufaro MC, Ciccocioppo F, Ronci M, et al. Proteomics characterization of extracellular vesicles sorted by flow cytometry reveals a disease-specific molecular cross-talk from cerebrospinal fluid and tears in multiple sclerosis. J Proteomics. 2019;204: 103403.
31. Hu L, Liu X, Zheng Q, Chen W, Xu H, Li H, et al. Interaction network of extracellular vesicles building universal analysis via eye tears: iNEBULA. Sci Adv. 2023;9: eadg1137.
32. Filippi M, Amato MP, Centonze D, Gallo P, Gasperini C, Inglese M, et al. Correction to: early use of high-efficacy disease-modifying therapies makes the difference in people with multiple sclerosis: an expert opinion. J Neurol. 2022;269:6690–1.
33. Rossi C, Cicalini I, Cufaro MC, Agnifili L, Mastropasqua L, Lanuti P, et al. Multi-omics approach for studying tears in treatment-naïve glaucoma patients. Int J Mol Sci. 2019;20:4029.
34. Cossarizza A, Chang H-D, Radbruch A, Acs A, Adam D, Adam-Klages S, et al. Guidelines for the use of flow cytometry and cell sorting in immunological studies (second edition). Eur J Immunol. 2019;49:1457–973.
35. Catitti G, De Bellis D, Vespa S, Simeone P, Canonico B, Lanuti P. Extracellular vesicles as players in the anti-inflammatory inter-cellular crosstalk induced by exercise training. Int J Mol Sci. 2022;23:14098.
36. Potenza F, Cufaro MC, Di Biase L, Panella V, Di Campli A, Ruggieri AG et al. Proteomic analysis of Marinesco-sjogren syndrome fibroblasts indicates pro-survival metabolic adaptation to SIL1 Loss. Int J Mol Sci. 2021;22:12449.
37. Simeone P, Celia C, Bologna G, Ercolino E, Pierdomenico L, Cilurzo F, et al. Diameters and fluorescence calibration for extracellular vesicle analyses by flow cytometry. Int J Mol Sci. 2020;21:7885.
38. Welsh JA, Van Der Pol E, Arkesteijn GJA, Bremer M, Brisson A, Coumans F, et al. MIFlowCyt-EV: a framework for standardized reporting of extracellular vesicle flow cytometry experiments. J Extracell Vesicles. 2020;9:1713526.
39. Correction to "Minimal information for studies of extracellular vesicles (MISEV2023): From basic to advanced approaches". J Extracell Vesicles. 2024;13:e12451.
40. Théry C, Witwer KW, Aikawa E, Alcaraz MJ, Anderson JD, Andriantsitohaina R, et al. Minimal information for studies of extracellular vesicles 2018 (MISEV2018): a position statement of the International Society for Extracellular Vesicles and update of the MISEV2014 guidelines. J Extracell Vesicles. 2018;7:1535750.
41. Brocco D, Simeone P, Buca D, Di MP, De Tursi M, Grassadonia A, et al. Blood circulating CD133+ extracellular vesicles predict clinical outcomes in patients with metastatic colorectal cancer. Cancers. 2022;14:1357.
42. Lanuti P, Simeone P, Rotta G, Almici C, Avvisati G, Azzaro R, et al. A standardized flow cytometry network study for the assessment of circulating endothelial cell physiological ranges. Sci Rep. 2018;8:5823.

43. Damiani V, Cufaro MC, Fucito M, Dufrusine B, Rossi C, Del Boccio P, et al. Proteomics approach highlights early changes in human fibroblasts-pancreatic ductal adenocarcinoma cells crosstalk. Cells. 2022;11:1160.
44. Madonna R, Pieragostino D, Cufaro MC, Del Boccio P, Pucci A, Mattii L, et al. Sex-related differential susceptibility to ponatinib cardiotoxicity and differential modulation of the Notch1 signalling pathway in a murine model. J Cell Mol Med. 2022;26:1380–91.
45. Lim MY, Paulo JA, Gygi SP. Evaluating false transfer rates from the match-between-runs algorithm with a two-proteome model. J Proteome Res. 2019;18:4020–6.
46. Kramer A, Green J, Pollard J Jr, Tugendreich S. Causal analysis approaches in ingenuity pathway analysis. Bioinformatics. 2014;30:523–30.
47. Perez-Riverol Y, Bai J, Bandla C, García-Seisdedos D, Hewapathirana S, Kamatchinathan S, et al. The PRIDE database resources in 2022: a hub for mass spectrometry-based proteomics evidences. Nucleic Acids Res. 2022;50:D543–52.
48. Zaru R, Orchard S, UniProt Consortium. UniProt tools: BLAST, align, peptide search, and ID mapping. Curr Protoc. 2023;3: e697.
49. Kalra H, Simpson RJ, Ji H, Aikawa E, Altevogt P, Askenase P, et al. Vesiclepedia: a compendium for extracellular vesicles with continuous community annotation. PLoS Biol. 2012;10: e1001450.
50. Pathan M, Keerthikumar S, Chisanga D, Alessandro R, Ang C, Askenase P, et al. A novel community driven software for functional enrichment analysis of extracellular vesicles data. J Extracell Vesicles. 2017;6:1321455.
51. Chitti SV, Gummadi S, Kang T, Shahi S, Marzan AL, Nedeva C, et al. Vesiclepedia 2024: an extracellular vesicles and extracellular particles repository. Nucleic Acids Res. 2024;52:D1694–8.
52. Van Deun J, Mestdagh P, Agostinis P, Akay Ö, Anand S, Anckaert J, et al. EV-TRACK: transparent reporting and centralizing knowledge in extracellular vesicle research. Nat Methods. 2017;14:228–32.
53. Brocco D, Lanuti P, Simeone P, Bologna G, Pieragostino D, Cufaro MC, et al. Corrigendum to "Circulating Cancer Stem Cell-Derived Extracellular Vesicles as a Novel Biomarker for Clinical Outcome Evaluation." J Oncol. 2020;2020:8947367.
54. Catitti G, Cufaro MC, De Bellis D, Cicalini I, Vespa S, Tonelli F, et al. Extracellular vesicles in regenerative processes associated with muscle injury recovery of professional athletes undergoing sub maximal strength rehabilitation. Int J Mol Sci. 2022;23:14913.
55. Yates AG, Pink RC, Erdbrügger U, Siljander PR-M, Dellar ER, Pantazi P, et al. In sickness and in health: The functional role of extracellular vesicles in physiology and pathology in vivo: Part I: Health and Normal Physiology: Part I: Health and Normal Physiology. J Extracell Vesicles. 2022;11: e12151.
56. Rheinländer A, Schraven B, Bommhardt U. CD45 in human physiology and clinical medicine. Immunol Lett. 2018;196:22–32.
57. Corrado C, Barreca MM, Zichittella C, Alessandro R, Conigliaro A. Molecular mediators of RNA loading into extracellular vesicles. Cells. 2021;10:3355.
58. Fabbiano F, Corsi J, Gurrieri E, Trevisan C, Notarangelo M, D'Agostino VG. RNA packaging into extracellular vesicles: an orchestra of RNA-binding proteins? J Extracell Vesicles. 2020. https://doi.org/10.1002/jev2.12043.
59. Minagar A, Maghzi AH, McGee JC, Alexander JS. Emerging roles of endothelial cells in multiple sclerosis pathophysiology and therapy. Neurol Res. 2012;34:738–45.
60. Correale J, Villa A. The blood–brain-barrier in multiple sclerosis: functional roles and therapeutic targeting. Autoimmunity. 2007;40:148–60.
61. Lopes Pinheiro MA, Kooij G, Mizee MR, Kamermans A, Enzmann G, Lyck R, et al. Immune cell trafficking across the barriers of the central nervous system in multiple sclerosis and stroke. Biochimica et Biophysica Acta BBA Mol Basis Dis. 2016;1862:461–71.
62. Ribatti D, Tamma R, Annese T. Mast cells and angiogenesis in multiple sclerosis. Inflamm Res. 2020;69:1103–10.
63. Kirk S, Frank JA, Karlik S. Angiogenesis in multiple sclerosis: is it good, bad or an epiphenomenon? J Neurol Sci. 2004;217:125–30.
64. Girolamo F, Coppola C, Ribatti D, Trojano M. Angiogenesis in multiple sclerosis and experimental autoimmune encephalomyelitis. Acta Neuropathol Commun. 2014;2:84.
65. Tóth EÁ, Turiák L, Visnovitz T, Cserép C, Mázló A, Sódar BW, et al. Formation of a protein corona on the surface of extracellular vesicles in blood plasma. J Extracell Vesicles. 2021. https://doi.org/10.1002/jev2.12140.
66. Liam-Or R, Faruqu FN, Walters A, Han S, Xu L, Wang JT-W, et al. Cellular uptake and in vivo distribution of mesenchymal-stem-cell-derived extracellular vesicles are protein corona dependent. Nat Nanotechnol. 2024;19:846–55.

Publisher's Note